Biochemistry

pubs.acs.org/biochemistry Article

The Expression of Human DNA Helicase B Is Affected by G-Quadruplexes in the Promoter

Maroof Khan Zafar, Lindsey Hazeslip, Muhammad Zain Chauhan, and Alicia K. Byrd*

Cite This: *Biochemistry* 2020, 59, 2401−2409 Read Online

ACCESS | Metrics & More | Article Recommendations | Supporting Information

ABSTRACT: G-Quadruplexes are secondary structures that can form in guanine-rich DNA and RNA that have been implicated in regulating multiple biological processes, including transcription. G-Quadruplex-forming sequences are prevalent in promoter regions of proto-oncogenes and DNA repair proteins. HELB is a human helicase involved in DNA replication and repair with 12 runs of three to four guanines in the proximal promoter. This sequence has the potential to form three canonical three-tetrad G-quadruplexes. Our results show that although all three G-quadruplexes can form, a structure containing two noncanonical G-quadruplexes with longer loops containing runs of three to four guanines is the most prevalent. These *HELB* G-quadruplexes are stable under physiological conditions. In cells, stabilization of the G-quadruplexes results in a decrease in the level of HELB expression, suggesting that the G-quadruplexes in the *HELB* promoter serve as transcriptional repressors.

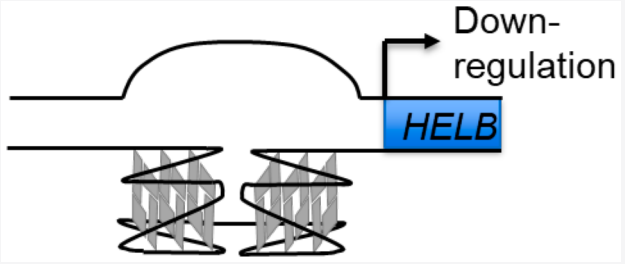

G-Quadruplexes (G4DNA) are four-stranded structures that can form in guanine-rich nucleic acid sequences with the consensus motif $G_3N_{1-7}G_3N_{1-7}G_3N_{1-7}G_3$.[1,2] Interactions of four guanines through Hoogsteen hydrogen bonding form a tetrad (Figure 1A). Stacking of multiple tetrads stabilized by monovalent cations in the central channel forms the G4DNA structure (Figure 1B). K^+ and Na^+ both stabilize G4DNA structures by coordinating the O6 atoms lining the central channel, although K^+ results in G4DNA structures that are more stable than those with Na^+.[1,3] The small radius of Li^+ results in poor coordination of the O6 and minimal induction of G4 folding.[4] The stability of G4DNA sequences *in vitro* is dependent on the number of tetrads and the length of the intervening loops.[2] Increasing the number of tetrads and decreasing the loop length result in a more stable structure. G4DNA sequences can also adopt several conformations. In a parallel structure, each of the strands is oriented in the same direction, whereas the orientation of each strand alternates in antiparallel G4DNA. Hybrid structures contain a combination of parallel and antiparallel strand orientations.

G4DNA has been visualized in cells using antibodies and small molecules,[5−8] and their locations in the genome have been mapped using sequencing.[9,10] These sequences are associated with common breakpoints in the mitochondrial genome[11,12] and with DNA breakpoints in cancer.[2] Putative G4DNA sequences are not randomly distributed in the genome. Instead, they are clustered in telomeres, rDNA, mtDNA, splice sites, replication origins, and promoters.[1,13−15] G4DNA sequences are enriched in the promoters of proto-oncogenes and DNA repair genes relative to tumor suppressors and housekeeping genes.[16−18] This nonrandom distribution suggests that G4DNA structures serve a functional role in the genome. Due to the prevalence of G4DNA sequences in the promoters of proto-oncogenes and their effect on gene expression, G4DNA structures are potential therapeutic targets.[19−22]

Expression of many proto-oncogenes such as c-MYC,[23] VEGF,[24] and KRAS[25] is affected by the G4DNA in the promoter. Two different quadruplexes can form in the nuclease hypersensitive element NHE III_1 upstream of the c-MYC P1 promoter, one of which controls 85−90% of the transcription of the c-MYC gene.[23] Expression of a reporter gene was shown to be affected by G4DNA sequences from DNA repair gene promoters when the G4DNA sequences were inserted upstream of the transcription start site (TSS).[18,26,27] However, expression of a DNA repair gene has not been directly shown to be affected by the formation of G4DNA in its promoter.

The *HELB* gene encodes the DNA repair protein DNA helicase B (HELB). HELB has been proposed to be involved in loading the preinitiation complex through its interaction with DNA polymerase α primase, CDC45, and TOPBP1 in the late G1 phase.[28,29] Additionally, HELB localized to chromatin in response to treatment with DNA-damaging agents such as camptothecin and etoposide.[30] HELB negatively regulates

Received: March 16, 2020
Revised: May 26, 2020
Published: June 1, 2020

https://dx.doi.org/10.1021/acs.biochem.0c00218
Biochemistry 2020, 59, 2401−2409

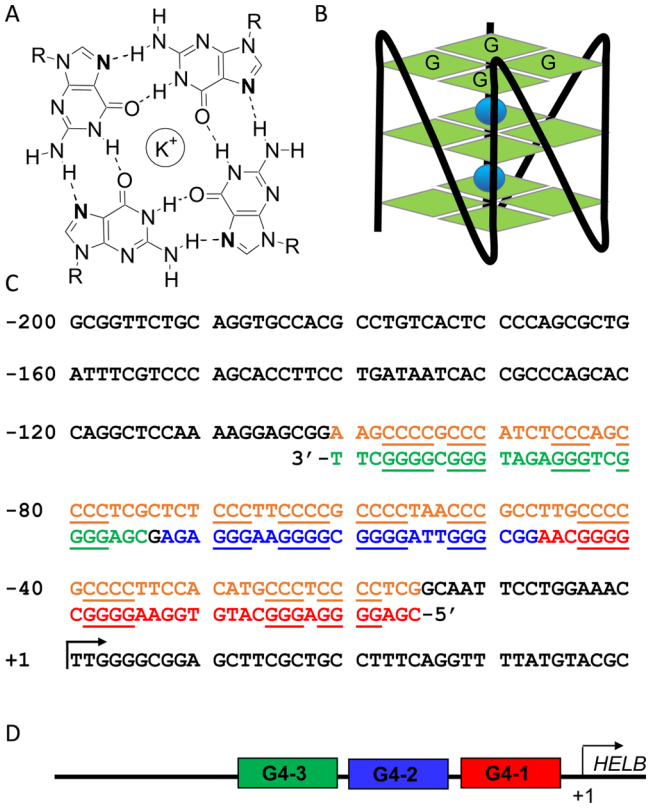

Figure 1. *HELB* promoter that contains putative G4DNA-forming sequences. (A) Four guanine residues can form a G-tetrad through Hoogsteen hydrogen bonding between N7 and O6 of one guanine and N1 and N2 of another guanine. The N7 atom that is protected in G4DNA but accessible in ssDNA and dsDNA is shown in bold. (B) Multiple G-tetrads can stack to form a G-quadruplex stabilized by monovalent cations in the central channel. (C) The *HELB* promoter contains a C-rich sequence (orange) just upstream of the TSS (arrow at +1). The reverse complement of the C-rich region contains three potential G4DNA-forming sequences (red, blue, and green). (D) The sequence closest to the TSS is HELB-G4-1, the middle HELB-G4-2, and the furthest upstream of the TSS HELB-G4-3.

DNA double-strand break repair by homologous recombination in the G1 phase by inhibiting end resection.[31] The *HELB* promoter contains a C-rich sequence on the coding strand in the 100 nucleotides upstream of the transcription start site (Figure 1C). The template strand (Figure 1C,D) has the potential to form three canonical three-tetrad G4DNA structures (red, blue, and green), while the coding strand (orange) could potentially form i-motifs (iM). Here we investigate the ability of these sequences to form secondary DNA structures and their effect on expression of *HELB*.

MATERIALS AND METHODS

Oligonucleotides, Proteins, Cells, and Antibodies. Oligonucleotides were ordered from Integrated DNA Technologies with desalting except for those used for DMS footprinting, which were ordered high-performance liquid chromatography-purified. Templates for polymerase extension assays were purified by denaturing polyacrylamide gel electrophoresis (PAGE) as described previously.[32] Oligonucleotide sequences are listed in Table S1. DNA Pol I from *Mycobacterium tuberculosis* (MtbPol I) was a kind gift from A. Ketkar and R. Eoff.[33,34] HEK 293T cells were cultured in DMEM with 10% EquaFetal and penicillin/streptomycin. HELB was detected using a rabbit polyclonal antibody from Abcam (ab202141) and a HRP-labeled goat anti-rabbit IgG from PerkinElmer (NEF812001). c-MYC was detected using a rabbit monoclonal antibody from Cell Signaling (D84C12) and a HRP-labeled goat anti-rabbit IgG from PerkinElmer (NEF812001). The mouse β-actin antibody was purchased from Cell Signaling (8H10D10), and the HRP-labeled goat anti-mouse IgG from PerkinElmer (NEF822001).

Circular Dichroism (CD). Oligonucleotides (Table S1) were resuspended at 5 μM in 10 mM Tris-HCl (pH 7.5) and 140 mM KCl or LiCl. To test G4DNA formation, samples were heated to 95 °C for 10 min and slowly cooled to room temperature. To test i-motif (iM) formation, oligonucleotides containing the potential iM (Table S1) were resuspended at 5 μM in phosphate buffers at pH 5.5, 6.5, and 7.5. Circular dichroism was measured using a Jasco J-1100 CD spectrometer at 25 °C. The spectrum of buffer lacking DNA was subtracted, and data were smoothed using the Savitzky–Golay method and converted to molar ellipticity.

T_m Measurement. Oligonucleotides were prepared as described for circular dichroism, and the T_m was determined by measuring the change in the molar ellipticity at 265 nm for G4DNA and at 290 nm for iM as the temperature increased from 4 to 95 °C at a rate of 1 °C/min in a Jasco J-1100 CD spectrometer. Data were normalized and fit to the inhibitor versus response variable slope (four parameters) using GraphPad Prism 8.2.

DMS Footprinting. Dimethyl sulfate (DMS) was diluted to 20% in ethanol immediately before use. 5′-FAM-HELB-G4-123-Bio-3′ (Table S1) at 100 nM in 25 mM Tris-HCl (pH 7.5) and 140 mM KCl or LiCl with 3.3 ng/μL salmon sperm DNA was incubated for 5 s with 0.4% DMS before the reaction was quenched with 1 M BME and 13.2 mM EDTA (final concentrations). The DNA was captured by adding streptavidin M-280 Dynabeads to a final concentration of 0.4 ng/μL. The captured DNA was cleaved by resuspension in 1 M piperidine and 0.1 mM biotin and heating at 95 °C for 30 min. The samples were dried and resuspended in 95% formamide, 20 mM EDTA, and bromophenol blue before being heated at 95 °C for 10 min. Samples were separated on a 10% polyacrylamide–7 M urea gel. Samples were visualized using a Typhoon Trio Imager (GE Healthcare) using a 488 nm laser and a 520 nm bandpass 40 emission filter. Quantification is the intensity of a line half the width of the lane determined using FIJI.

Polymerase Stop. The HELB-G4 template (Table S1) was annealed by mixing with fluorescein-labeled 25-mer primer (5 μM each) in 50 mM Tris-HCl (pH 7.5) and 100 mM KCl or LiCl, heating for 10 min at 95 °C, and slowly cooling to room temperature. The substrate (200 nM) was mixed with 10 nM Pol I from *M. tuberculosis* (MtbPol I) in the presence of 50 mM Tris-HCl (pH 7.5), 100 mM KCl or LiCl, 1% glycerol, 5 mM DTT, and 0.1 mg/mL BSA. The reaction was initiated by adding 250 μM dNTPs and 5 mM $MgCl_2$. The reactions were quenched at various times with 95% formamide, 20 mM EDTA, and bromophenol blue before the mixtures were heated at 95 °C for 5 min. Samples were resolved by loading 150 fmol of DNA on a 10% polyacrylamide–7 M urea gel. The gel was visualized with a Typhoon Trio Imager (GE Healthcare) using a 488 nm laser and a 520 nm bandpass 40 emission filter. The intensity of product bands was quantified using ImageQuant TL (GE Healthcare).

https://dx.doi.org/10.1021/acs.biochem.0c00218
Biochemistry 2020, 59, 2401–2409

Quantitative Reverse Transcription Polymerase Chain Reaction (PCR). HEK 293T cells treated with 100 μM TMPyP4 for 48 h before being harvested were compared to untreated HEK 293T cells. RNA was isolated using a RNeasy kit (Qiagen). RNA was quantified using a NanoDrop 2000C instrument (Thermo Scientific). DNase digestion was performed on 1 μg of isolated RNA with 1 unit of RQ1 RNase-free DNase (Promega) in 1× RQ1 RNase-free DNase reaction buffer at 37 °C for 30 min. cDNA was synthesized with an iScript cDNA Synthesis Kit (BioRad) following the manufacturer's recommended protocol in a 20 μL reaction mixture with synthesis for 5 min at 25 °C, 20 min at 46 °C, and 1 min at 95 °C. cDNA was amplified using Sso Advanced Universal SYBR Green Supermix (Bio-Rad) with 300 nM forward and reverse primers (Table S2) in a Bio-Rad CFX96 Real Time PCR Machine. Each reaction mixture (20 μL) contained 2 μL of template. The PCR cycle was one cycle of 98 °C for 3 min and 40 cycles of 98 °C for 15 s and 53 °C for 30 s, followed by a melt curve from 65 to 90 °C to determine specificity. Information about the amplicons is available in Table S3. Experiments were performed in biological and technical triplicates. The fold change in expression was calculated using the ΔC_t method[35] with $\Delta C_t = C_{t_{target}} - C_{t_{ref}}$. The $2^{-\Delta C_t}$ values were averaged and normalized to β-actin, and significance was determined using GraphPad Prism 8.2 to perform a two-tailed t test.

Western Blot. HEK 293T cells were treated with TMPyP4 or PDS for 48 h before being harvested. The cells were lysed in 40 mM HEPES (pH 7.5), 10 mM NaCl, and 1% Triton X-100 in the presence of protease inhibitor cocktail (Sigma, catalog no. P2714), 1 mM DTT, 1 mM sodium orthovanadate, and 20 mM β-glycerophosphate; 40 μg of whole cell lysate was loaded on 4−15% Mini-PROTEAN TGX stain-free gels to separate the proteins. The proteins were transferred to a 0.45 μm nitrocellulose membrane and probed with primary antibodies against HELB (1:10000), c-MYC (1:2000), and β-actin (1:2000), followed by HRP-conjugated secondary antibodies (1:5000). The signal was developed with ECL Prime Western Blotting Detection Reagent (GE Healthcare Amersham) and imaged using Bio-Rad ChemiDoc MP.

Luciferase Assay. HEK 293T cells were transfected with Lipofectamine 3000 (Invitrogen) in a 96-well plate. A total of 8 × 10^3 cells/well were plated in a white flat bottom plate (PerkinElmer) and transfected with 100 ng per well of firefly luciferase reporter plasmid containing a portion of the *HELB* promoter and 50 ng per well of pRL-TK Renilla luciferase control plasmid for 24 h. Firefly luciferase plasmids were pGL4-HELB+G4 Extended containing residues −657 to +209 of the *HELB* promoter (pGL4-HDHB in ref 36), pGL4-HELB +G4 containing residues −152 to +209 of the *HELB* promoter (pGL4-HDHBδ2 in ref 36), or pGL4-HDHB-G4 containing residues +61 to +209 of the HELB promoter (pGL4-HDHBδ4 in ref 36). pGL4-HELB+G4 and pGL4-HELB+G4 Extended both contain the G4DNA-forming region in the *HELB* promoter. pGL4-HELB-G4 lacks the G4DNA-forming region. Firefly luciferase plasmids were a kind gift from F. Uchiumi.[36] After transfection, cells were treated with 100 μM TMPyP4 for 24 h. Firefly luminescence and Renilla luminescence were measured with the Dual-Glo Luciferase Assay (Promega) according to the manufacturer's protocol using a PerkinElmer Victor Nivo instrument. The ratio of the luminescence from the firefly plasmid relative to the Renilla plasmid was calculated. The relative luminescence of the treated samples was normalized to the relative luminescence of the untreated samples.

RESULTS

Three G4DNA Structures Can Form in the *HELB* Promoter. The region immediately upstream of the TSS in the *HELB* gene is highly GC-rich with a C-rich coding strand and a G-rich template strand that have the potential to form iM and G4DNA structures, respectively (Figure 1). Twelve runs of C/G are present in this region, potentially allowing formation of three iM and/or G4DNA structures. To test the ability of these structures to form, CD of oligonucleotides containing the first four runs of Cs/Gs [HELB-iM-1/HELB-G4-1 (red in Figure 1)], the middle four runs of Cs/Gs [HELB-iM-2/HELB-G4-2 (blue in Figure 1)], and the furthest upstream four runs of Cs/Gs [HELB-iM-3/HELB-G4-3 (green in Figure 1)] was measured. All three G4DNA sequences formed parallel G4DNA structures at physiological pH and K^+ concentration (Figure 2A) as indicated by the ellipticity

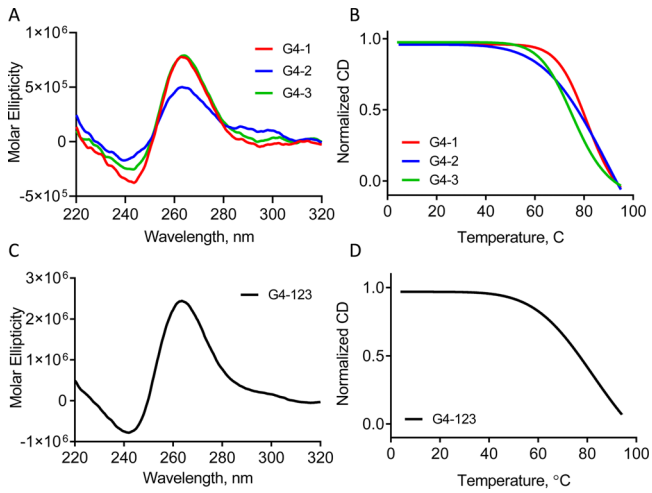

Figure 2. All three of the G4DNA sequences form parallel G-quadruplexes. (A) Circular dichroism spectroscopy of each of the G4DNA sequences individually indicates that they each form a parallel G4DNA structure. (B) Melting temperature measurement by CD indicates that the T_m values of HELB-G4-1, HELB-G4-2, and HELB-G4-3 are at least 75 °C. The T_m values are not defined because the G4 structures were not completely melted by the end of the measurement at 95 °C. (C) The CD spectrum of the entire G-rich sequence containing all three G4DNA sequences indicates formation of a parallel quadruplex. (D) The melting temperature of the entire G-rich sequence determined by CD is at least 75 °C.

maxima at 265 nm and minima at 240 nm. HELB-G4-2 may form a small amount of antiparallel or hybrid quadruplex based on the small peak present around 290 nm. However, this sequence predominately folds into a parallel quadruplex. Each of the G4DNA structures has a melting temperature above 75 °C (Figure 2B). The CD spectra in Li^+ indicate a reduced level of G4 formation relative to that in K^+ (Figure S1A−C). All three iM sequences formed iM structures at pH 5.5, but not at higher pH values (Figure S2A−C). The melting temperatures of the three iM structures were 30−40 °C at pH 5.5 (Figure S1D).

The sequences do not exist in isolation in the HELB promoter, so the ability of an oligonucleotide containing all 12

https://dx.doi.org/10.1021/acs.biochem.0c00218
Biochemistry 2020, 59, 2401−2409

runs of Cs/Gs (HELB-iM-123/HELBG4-123) to form structures was measured. The full G-rich sequence formed a parallel quadruplex with a molar ellipticity that was higher than those of the three individual G4DNA structures (Figure 2C) that was greatly reduced in Li^+ (Figure S1D). The melting temperature in K^+ is >75 °C (Figure 2D). The full C-rich sequence formed an iM structure at pH 5.5 with a molar ellipticity that was higher than those of the three individual iM structures (Figure S2E) with a melting temperature of 42 °C (Figure S2F). Because the G4DNA structures are highly stable at physiological pH, salt concentration, and temperature and the iM structures are not stable under these conditions, we chose to continue our studies with only the G4DNA structures, as they are likely to be more physiologically relevant.

Guanines in Eight of the Twelve G-Runs Are Involved in G4 Formation. DMS is an alkylating agent that preferentially alkylates the N7 position of guanine. N7 of guanine is accessible in both ssDNA and duplex DNA but is inaccessible in G4DNA due to hydrogen bonding with the exocyclic N2 atom of an adjacent guanine (Figure 1A). Thus, DMS footprinting can be used to determine which guanine residues are involved in G4DNA formation. DMS footprinting of the full G-rich sequence from the HELB promoter results in less reactive DNA in K^+ than in Li^+, indicating that G4DNA structures are indeed forming (Figure 3). Three of the four G-runs labeled as G4-3 in Figure 1 are protected, as are three of the four G-runs from G4-1. Two of the G-runs from G4-2 are protected for a total of eight protected G-runs. This indicates that although three G4DNA structures can form in the HELB promoter, two G4DNA structures are more likely to form *in vitro*. It should be noted that a small degree of protection of all G-runs except number 10 in G4-3 was observed, indicating that there is likely some variability in the G-runs involved in G4DNA formation. The G-runs that are most protected are those that are most often involved in G4DNA formation. Surprisingly, the G4DNA structures formed are not those with the shortest possible loops.

The protection pattern observed in DMS footprinting was confirmed with targeted mutagenesis. All of the guanines in the G-runs were replaced with adenines (Figure 4A and Table S1) because adenine is also a purine but is unable to form Hoogsteen hydrogen bonds with itself, and therefore unable to support G4DNA formation.[37] As expected, these mutated G4DNA sequences do not fold into G4DNA structures (Figure 4B, green). An oligonucleotide with mutations in G-runs that were protected in K^+ from reaction with DMS was also not able to form a G4DNA structure (Figure 4B, orange). On the other hand, an oligonucleotide with mutations in the G-runs that were reactive with DMS in K^+ was able to form a G4DNA structure (Figure 4B, blue). The secondary structure that formed in the oligonucleotide with the protected guanines mutated was very unstable (Figure 4C, orange), whereas the parallel G4DNA structure formed with the reactive guanines mutated melted at a temperature similar to that of the unmodified sequence (blue vs black in Figure 4C). The melting transition was more extended for the unmodified sequence, indicating that there are likely multiple different structures that form in the full-length G-rich sequence. However, on the basis of the DMS footprinting results and the melting curves, we can conclude that the predominant G4DNA structure formed *in vitro* in the HELB promoter contains two parallel quadruplexes formed from G-runs 1, 2, 4, 7–9, 11, and 12 from the 5′-end corresponding to three G-runs from G4DNA-1, two G-runs from G4DNA-2, and three G-runs from G4DNA-3.

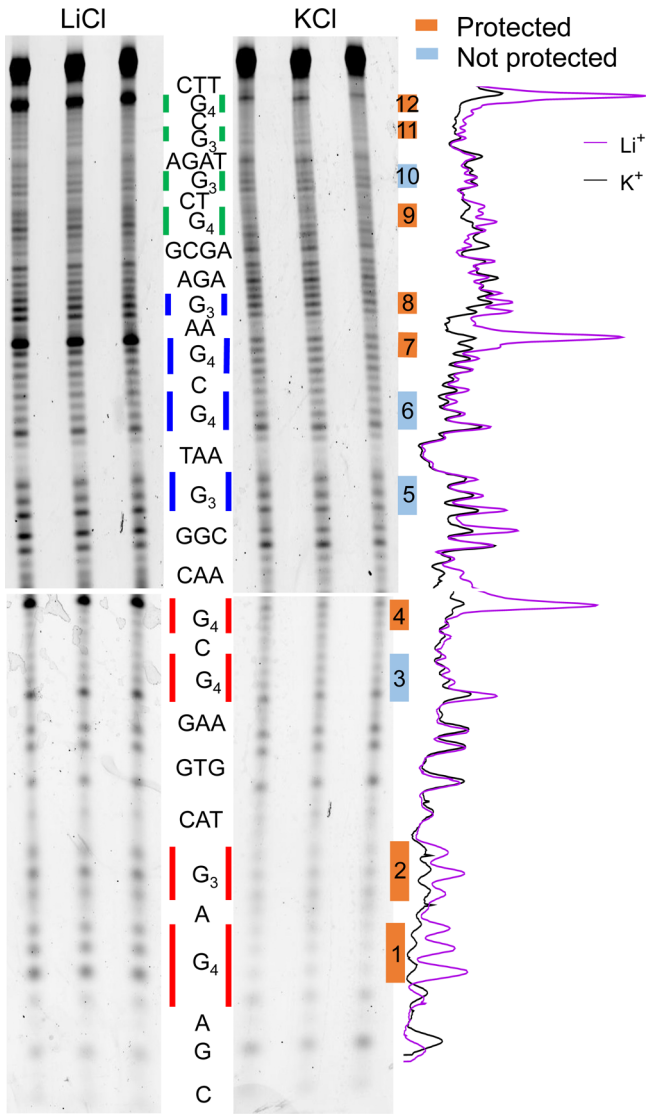

Figure 3. DMS footprinting of the biotinylated G-rich sequence in buffer containing Li^+ or K^+ indicates guanine residues are protected in K^+. The oligonucleotide sequence is given in the middle, and each of the G-runs is shaded in the middle to indicate whether they come from G4-1 (red), G4-2 (blue), or G4-3 (green). We were unable to separate all 86 nucleotides on a single gel so samples were loaded onto two separate 10% polyacrylamide−7 M urea gels. One was run for 12 h to resolve the larger products, and one was run for 10 h to resolve the smaller species. The intensities of each lane were determined by FIJI and averaged and are plotted on the right. G-Runs that are protected in K^+ are marked with orange bars. Those that are not protected are marked with light blue bars. G-Runs are numbered from 5′ to 3′.

G4DNA structures can be an obstacle to DNA synthesis, which can result in DNA breakage *in vivo*.[2,11,12] This blockage of synthesis also serves as a useful tool for studying G4DNA *in vitro*.[38,39] The guanines at the 3′-end of the sequence are the most difficult to resolve in the DMS footprinting due to their location at the top of the gel where the separation between each cleaved oligonucleotide is the smallest. Therefore, to obtain more information about the involvement of guanine

https://dx.doi.org/10.1021/acs.biochem.0c00218
Biochemistry 2020, 59, 2401−2409

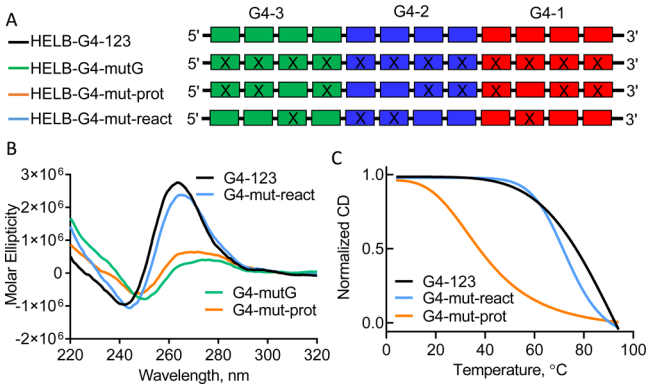

Figure 4. Mutation of reactive guanine bases does not affect G4DNA formation. (A) This diagram shows the individual G-runs as boxes colored to match the three individual G4 sequences as in Figure 1. Boxes with an x have guanines mutated to adenine (sequences in Table S1). (B) Mutation of all G-runs in the *HELB* promoter G-rich sequence or mutation of all protected guanines eliminates G4DNA formation (green or orange, respectively). An oligonucleotide with guanine residues that were reactive in K^+ mutated folds into a parallel G4DNA structure (blue) similar to the wild type sequence (black). (C) Melting temperature measurement by CD of oligonucleotides with no mutations (black), reactive guanines mutated (blue), and protected guanines mutated (orange) indicates T_m values were >75, 73, and 39 °C, respectively. The T_m for the unmodified sequence was not defined due to the lack of complete melting at 95 °C.

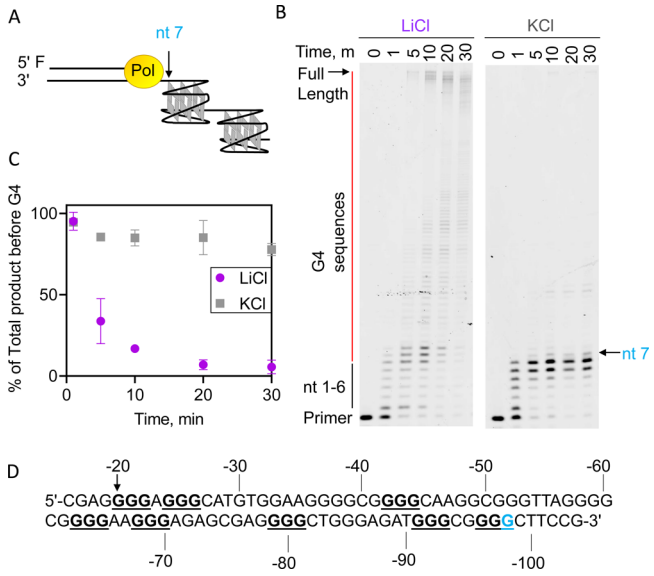

Figure 5. Polymerase stop assay that indicates polymerase stalling at HELB G4DNA. (A) Illustration of the substrate containing a primer hybridized to a template containing the G-rich region from the *HELB* promoter. The first guanine is seven nucleotides from the double-strand−single-strand junction (cyan). Reactions were performed in KCl or LiCl. (B) Products are separated by denaturing PAGE, and quantitation of the percent of product before the G-rich region (nucleotides 1−6) relative to total product (C) indicates stalling at the first G4DNA guanine in K^+. (D) Guanines in the *HELB* proximal promoter involved in G4DNA formation based on DMS footprinting and polymerase stop assays are underlined. Nucleotide 7 at which the stalling occurs in the polymerase assay in KCl is colored cyan.

residues at the 3′-end of the HELB G4DNA-forming sequence, a polymerase stop assay was performed. This experiment relies on the ability of a G4DNA structure to block synthesis by a polymerase and is used to determine the presence of and, to some degree, the stability of a G4DNA structure.[23,39] An oligonucleotide containing a 3′-tail on the G-rich region from the *HELB* promoter was annealed to an oligonucleotide complementary to a portion of the 3′-tail to produce a substrate with a six-nucleotide gap between the primer−template junction and the first guanine of HELB-G4-123 (Figure 5A). The polymerase was able to synthesize into the G-rich sequence in Li^+ to a much greater extent than in K^+ (Figure 5B). In K^+, 80% of DNA synthesis was stalled before the quadruplex at nucleotides 5 and 6 (Figure 5C). The base at position 7 is the first guanine of the G4DNA-forming region. This indicates that the majority of the substrate was involved in formation of a stable G4DNA structure and that the 3′-guanine is involved in G4DNA formation in the context of the entire G-rich sequence. On the basis of the combination of DMS footprinting (Figure 3) and the polymerase stop assay (Figure 5A−C), we can define the guanine residues in the HELB promoter most involved in the formation of G4DNA structures *in vitro* (Figure 5D).

G4DNA Binding Compounds Decrease the Level of Expression of HELB. Because G4DNA structures in promoters have been shown to regulate gene expression, the expression of HELB in the presence of the G4DNA-stabilizing agent TMPyP4 was measured. The quantity of *HELB* mRNA was decreased in the presence of TMPyP4, although not to the degree that the level of expression of *c-MYC* was decreased (Figure 6A). Because 85−90% of the transcription of the *c-MYC* gene is controlled by the G4DNA sequence at NHE III_1,[23] this is not surprising. The level of transcription of *HELB* was decreased ∼35% upon treatment with TMPyP4. To determine whether G4DNA stabilization affected the quantity of HELB protein present, Western blotting was used to determine the level of HELB protein in the presence and absence of TMPyP4 (Figure 6B) and pyridostatin (PDS) (Figure 6C). In both cases, the quantity of HELB protein was reduced ∼50% in the presence of the G4DNA-stabilizing agents (Figure 6D). Expression of *β*-actin that does not contain a G4DNA sequence in its promoter was unchanged upon treatment with either G4DNA-stabilizing agent. These results suggest that the G4DNA sequences in the *HELB* promoter may serve a regulatory role.

To confirm that the decrease in the level of expression was due to G4DNA stabilization, we measured expression of a luciferase reporter gene containing portions of the *HELB* promoter either containing (pGL4-HELB+G4 and pGL4-HELB+G4 Extended) or lacking (pGL4-HELB-G4) the G4DNA-forming region in the presence of TMPyP4 (Figure 6E). Luciferase activity with the pGL4-HELB+G4 and pGL4-HELB+G4 Extended constructs containing the G4DNA-forming region from the *HELB* promoter was sensitive to TMPyP4, while activity with the pGL4-HELB-G4 construct lacking the G4DNA-forming region was not sensitive to TMPyP4. This indicates that the changes in HELB expression observed upon addition of G4DNA-stabilizing compounds are indeed due to formation of G4DNA structures.

DISCUSSION

G4DNA structures in promoters can regulate gene expression. In fact, the prevalence of G4DNA structures that modulate expression in the promoters of proto-oncogenes has generated interest in therapies targeting these G4DNA structures.[20−22] The Burrows lab recently published a bioinformatics analysis

https://dx.doi.org/10.1021/acs.biochem.0c00218
Biochemistry 2020, 59, 2401−2409

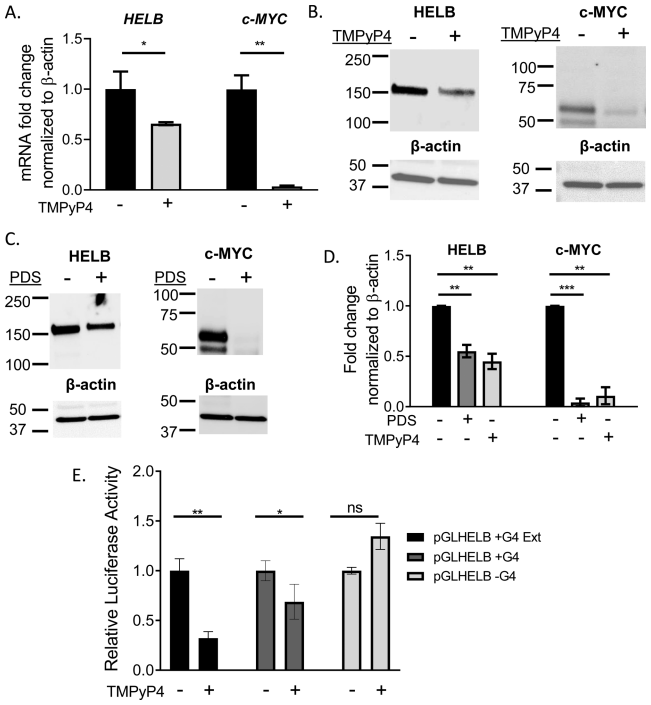

Figure 6. HELB expression is inhibited in the presence of G4DNA stabilizers. (A) RT-qPCR of *HELB* and *c-MYC* gene expression in the presence and absence of TMPyP4 (48 h at 100 μM) plotted relative to β-actin. Western blot for HELB and c-MYC expression in the presence and absence of (B) 100 μM TMPyP4 or (C) 50 μM PDS is quantified relative to β-actin in panel D. (E) Plasmids encoding firefly luciferase contain a portion of the *HELB* promoter. pGL4-HELB+G4 contains the entire G4DNA-forming region, and pGL4-HELB-G4 lacks the G4DNA-forming region. pGL4-HELB+G4 Extended contains the G4DNA-forming region and 500 bp upstream. Expression of firefly luciferase relative to a Renilla luciferase control plasmid is normalized to expression in the absence of TMPyP4. Data are the average and standard deviation of biological triplicate experiments. On the basis of a two-tailed *t* test, $*p < 0.05$, $**p < 0.01$, and $***p < 0.001$.

showing that DNA repair proteins are also enriched in G4DNA sequences in their promoters and 5′-UTRs.[18] Interestingly, expression of many DNA repair genes has been shown to be modulated by oxidative stress.[40,41] Formation of 8-oxo-7,8-dihydroguanine (8-oxoG) in the G4DNA in the *VEGF*,[26] *NTHL1*,[26] *PCNA*,[42] and *SIRT1*[43] promoters results in an increased level of gene expression. During repair of 8-oxoG, an abasic site is produced by OGG1 that results in an increase in the level of G4DNA formation due to destabilization of the duplex.[44] This suggests a mechanism for regulation of expression of some genes involved in DNA repair through formation of G4DNA in response to oxidative stress.

HELB is a helicase involved in DNA repair.[30,31] Here we have shown that three individual G4DNA structures can form in the promoter of the *HELB* gene (Figure 2). However, the most prevalent structure formed *in vitro* contains two G4DNA structures with longer loops (Figures 3 and 4). These G4DNA structures can stall DNA synthesis (Figure 5) and regulate expression of the *HELB* gene (Figures 6), suggesting that G4DNA structures also form *in vivo*. However, the preferred structure *in vivo* may vary from that determined here due to the presence of other components that affect G4DNA stability in the cell. Molecular crowding, DNA supercoiling, base modifications, the presence of a complementary strand, and the binding of histones and non-histone proteins can all affect G4DNA formation and stability.[45−47] If only a portion of the G-rich sequence is in a single-stranded form free from bound proteins, this would affect the G4 structure that formed *in vivo*. The Maizels lab identified the *HELB* promoter as a binding site of the XPB subunit of the TFIIH complex.[48] XPB is a helicase that binds G4DNA, and 40% of XPB binding sites are G4DNA sequences. The binding of XPB has been proposed to regulate transcription at G4DNA motifs,[48] which is consistent with our results that G4DNA in the *HELB* promoter regulates expression of HELB.

Interestingly, promoter G4DNA sequences can be transcriptionally activating or repressing. G4DNA structures on the template strand have been proposed to stall progression of the RNA polymerase, while G4DNA on the coding strand has been proposed to activate transcription by keeping the transcribed strand single-stranded.[14] This is consistent with results obtained by measuring expression of a reporter gene with a G4DNA sequence on the template or coding strand of the promoter.[18,49,50] The G4DNA structures on the template strand of the *HELB* promoter are also transcriptionally repressive (Figure 6). However, it is not always that simple because G4DNA structures themselves can bind proteins that activate or repress transcription and G4DNA can alter the ability of transcription factors to bind.[14] G4DNA on the nontemplate strand downstream of the transcription start site can also repress transcription by preventing reannealing of duplex DNA behind the polymerase and therefore increase the extent of formation of RNA:DNA hybrids[51] that have been shown to inhibit further rounds of transcription.[52]

In some promoters such as *BCL-2*, *KRAS*, and *hTERT*, multiple G4DNA sequences are clustered just upstream of the TSS[53−56] as they are in the *HELB* promoter. One well-characterized example is the *KIT* promoter that has three G4DNA sequences (K1, SP, and K2) within 200 nucleotides upstream of the TSS,[37] and the folding of one affects the folding of the other structures. The K1 and K2 sequences form parallel G4DNA structures, and the SP sequence forms an antiparallel G4DNA structure in isolation; however, in the context of the full sequence, SP also forms a parallel G4DNA structure. SP folds only in combination with K2, suggesting that study of the entire G4DNA-forming sequence is important. Like *KIT*, the G4DNA structures in the *HELB* promoter are influenced by the neighboring sequences. However, in the case of *HELB*, instead of one G4DNA structure affecting the propensity of another to form, the G4DNA structures are formed from G-runs spread out across the G-rich sequence.

It is somewhat surprising that the most prevalent G4DNA structures in the HELB promoter based on DMS footprinting (Figure 3) and polymerase stop (Figure 5) are not those with the shortest possible loop length. The structures formed in the *HELB* promoter are quite stable under physiological salt conditions (Figure 2). However, a shorter loop length tends to correlate with more stable G4DNA structures. Sequencing studies from the Balasubramanian lab have shown that our knowledge is lacking with regard to which G4DNA structures are likely to form; computational methods missed >50% of the G4DNAs that were detected by sequencing.[10] Many of these G4DNAs that were not predicted contained long loops and bulges. In addition, the Mergny lab found that as long as two loops were short, the third loop could be very long without affecting the overall stability of the G4DNA.[57] Therefore,

https://dx.doi.org/10.1021/acs.biochem.0c00218
Biochemistry 2020, 59, 2401−2409

maybe it should be expected that G4DNA structures will fold using noncontiguous runs of guanines. Both the thermodynamic stability and the kinetics of G4 folding and unfolding affect the overall stability of G4DNA structures.[58] A shorter loop length tends to correlate with faster folding kinetics,[59] but other factors such as salt and intermediates in the folding pathway also affect folding and unfolding kinetics.[3,60,61] Thus, the formation of G4DNA structures with long loops containing G-runs may be due to other factors in addition to thermodynamic stability such as the kinetics of folding and unfolding.

In addition to regulation at the transcriptional level as shown here, HELB is also regulated post-translationally. HELB is phosphorylated at the G1-S transition by CDK2/cyclin E, resulting in activation of a nuclear export sequence and relocalization of the majority of the protein to the cytosol.[30] HELB is also phosphorylated by ATM and ATR in response to ionizing radiation.[62] However, other sites of phosphorylation and ubiquitination have been detected on HELB by mass spectrometry,[63−65] indicating that other unknown mechanisms are also involved in regulating HELB activity. A combination of regulatory mechanisms, some of which are slower and function over a longer time frame, such as the transcriptional regulation shown here have the opportunity to regulate HELB by changing the protein level at different developmental stages, in different cell types, or during tumorigenesis. Other regulatory mechanisms like phosphorylation have the potential to rapidly modulate HELB activity with cell cycle or DNA damage. The lack of HELB can allow BRCA1 deficient cells to gain resistance to PARP inhibitors.[31] Thus, modulation of HELB transcription and the concomitant changes in protein level could have important cellular implications.

■ ASSOCIATED CONTENT

Supporting Information

The Supporting Information is available free of charge at https://pubs.acs.org/doi/10.1021/acs.biochem.0c00218.

Oligonucleotide sequences, primer sequences, RT-qPCR target information, HELB G4DNA CD spectra in Li^+, and HELB i-motif CD spectra (PDF)

Accession Codes

MtbPol1, P9WNU5.

■ AUTHOR INFORMATION

Corresponding Author

Alicia K. Byrd − *Department of Biochemistry and Molecular Biology, University of Arkansas for Medical Sciences, Little Rock, Arkansas 72205, United States; Winthrop P. Rockefeller Cancer Institute, Little Rock, Arkansas 72205, United States;* orcid.org/0000-0001-5484-0759; Email: akbyrd@uams.edu

Authors

Maroof Khan Zafar − *Department of Biochemistry and Molecular Biology, University of Arkansas for Medical Sciences, Little Rock, Arkansas 72205, United States*

Lindsey Hazeslip − *Department of Biochemistry and Molecular Biology, University of Arkansas for Medical Sciences, Little Rock, Arkansas 72205, United States*

Muhammad Zain Chauhan − *Department of Biochemistry and Molecular Biology, University of Arkansas for Medical Sciences, Little Rock, Arkansas 72205, United States*

Complete contact information is available at: https://pubs.acs.org/10.1021/acs.biochem.0c00218

Funding

This work was supported by the Winthrop P. Rockefeller Cancer Institute, the Arkansas Children's Research Institute Center for Translational Pediatric Research [National Institutes of Health (P20GM121293 to A. Tackett)], the Arkansas Biosciences Institute, the major research component of the Arkansas Tobacco Settlement Proceeds Act of 2000, and the University of Arkansas for Medical Sciences Vice Chancellor for Research. Funding for open access charge from the Arkansas Biosciences Institute.

Notes

The authors declare no competing financial interest.

■ ACKNOWLEDGMENTS

The authors thank Amit Ketkar and Robert Eoff at the University of Arkansas for Medical Sciences for the kind gift of MtbPol I and Fumiaki Uchiumi of the Tokyo University of Science for the kind gift of the luciferase reporter plasmids.

■ ABBREVIATIONS

G4DNA, G-quadruplex DNA; TSS, transcription start site; iM, i-motif; MtbPol I, DNA Pol I from *M. tuberculosis*; PDS, pyridostatin; DMS, dimethyl sulfate.

■ REFERENCES

(1) Hansel-Hertsch, R., Di Antonio, M., and Balasubramanian, S. (2017) DNA G-quadruplexes in the human genome: detection, functions and therapeutic potential. *Nat. Rev. Mol. Cell Biol. 18*, 279−284.

(2) Rhodes, D., and Lipps, H. J. (2015) G-quadruplexes and their regulatory roles in biology. *Nucleic Acids Res. 43*, 8627−8637.

(3) Byrd, A. K., Bell, M. R., and Raney, K. D. (2018) Pif1 helicase unfolding of G-quadruplex DNA is highly dependent on sequence and reaction conditions. *J. Biol. Chem. 293*, 17792−17802.

(4) Largy, E., Mergny, J.-L., and Gabelica, V. (2016) *Met. Ions Life Sci. 16*, 203−258.

(5) Biffi, G., Di Antonio, M., Tannahill, D., and Balasubramanian, S. (2014) Visualization and selective chemical targeting of RNA G-quadruplex structures in the cytoplasm of human cells. *Nat. Chem. 6*, 75−80.

(6) Biffi, G., Tannahill, D., McCafferty, J., and Balasubramanian, S. (2013) Quantitative visualization of DNA G-quadruplex structures in human cells. *Nat. Chem. 5*, 182−186.

(7) Rodriguez, R., Miller, K. M., Forment, J. V., Bradshaw, C. R., Nikan, M., Britton, S., Oelschlaegel, T., Xhemalce, B., Balasubramanian, S., and Jackson, S. P. (2012) Small-molecule-induced DNA damage identifies alternative DNA structures in human genes. *Nat. Chem. Biol. 8*, 301−310.

(8) Huang, W. C., Tseng, T. Y., Chen, Y. T., Chang, C. C., Wang, Z. F., Wang, C. L., Hsu, T. N., Li, P. T., Chen, C. T., Lin, J. J., Lou, P. J., and Chang, T. C. (2015) Direct evidence of mitochondrial G-quadruplex DNA by using fluorescent anti-cancer agents. *Nucleic Acids Res. 43*, 10102−10113.

(9) Lam, E. Y., Beraldi, D., Tannahill, D., and Balasubramanian, S. (2013) G-quadruplex structures are stable and detectable in human genomic DNA. *Nat. Commun. 4*, 1796.

(10) Chambers, V. S., Marsico, G., Boutell, J. M., Di Antonio, M., Smith, G. P., and Balasubramanian, S. (2015) High-throughput sequencing of DNA G-quadruplex structures in the human genome. *Nat. Biotechnol. 33*, 877−881.

(11) Bharti, S. K., Sommers, J. A., Zhou, J., Kaplan, D. L., Spelbrink, J. N., Mergny, J. L., and Brosh, R. M., Jr. (2014) DNA sequences proximal to human mitochondrial DNA deletion breakpoints

prevalent in human disease form G-quadruplexes, a class of DNA structures inefficiently unwound by the mitochondrial replicative Twinkle helicase. *J. Biol. Chem. 289*, 29975−29993.
(12) Dong, D. W., Pereira, F., Barrett, S. P., Kolesar, J. E., Cao, K., Damas, J., Yatsunyk, L. A., Johnson, F. B., and Kaufman, B. A. (2014) Association of G-quadruplex forming sequences with human mtDNA deletion breakpoints. *BMC Genomics 15*, 677.
(13) Maizels, N., and Gray, L. T. (2013) The G4 genome. *PLoS Genet. 9*, No. e1003468.
(14) Bochman, M. L., Paeschke, K., and Zakian, V. A. (2012) DNA secondary structures: stability and function of G-quadruplex structures. *Nat. Rev. Genet. 13*, 770−780.
(15) Falabella, M., Fernandez, R. J., Johnson, F. B., and Kaufman, B. A. (2019) Potential Roles for G-Quadruplexes in Mitochondria. *Curr. Med. Chem. 26*, 2918−2932.
(16) Eddy, J., and Maizels, N. (2006) Gene function correlates with potential for G4 DNA formation in the human genome. *Nucleic Acids Res. 34*, 3887−3896.
(17) Huppert, J. L., and Balasubramanian, S. (2007) G-quadruplexes in promoters throughout the human genome. *Nucleic Acids Res. 35*, 406−413.
(18) Fleming, A. M., Zhu, J., Ding, Y., Visser, J. A., Zhu, J., and Burrows, C. J. (2018) Human DNA Repair Genes Possess Potential G-Quadruplex Sequences in Their Promoters and 5′-Untranslated Regions. *Biochemistry 57*, 991−1002.
(19) Neidle, S. (2016) Quadruplex Nucleic Acids as Novel Therapeutic Targets. *J. Med. Chem. 59*, 5987−6011.
(20) Balasubramanian, S., Hurley, L. H., and Neidle, S. (2011) Targeting G-quadruplexes in gene promoters: a novel anticancer strategy? *Nat. Rev. Drug Discovery 10*, 261−275.
(21) Balasubramanian, S., and Neidle, S. (2009) G-quadruplex nucleic acids as therapeutic targets. *Curr. Opin. Chem. Biol. 13*, 345−353.
(22) De Cian, A., Lacroix, L., Douarre, C., Temime-Smaali, N., Trentesaux, C., Riou, J. F., and Mergny, J. L. (2008) Targeting telomeres and telomerase. *Biochimie 90*, 131−155.
(23) Siddiqui-Jain, A., Grand, C. L., Bearss, D. J., and Hurley, L. H. (2002) Direct evidence for a G-quadruplex in a promoter region and its targeting with a small molecule to repress c-MYC transcription. *Proc. Natl. Acad. Sci. U. S. A. 99*, 11593−11598.
(24) Sun, D., Liu, W. J., Guo, K., Rusche, J. J., Ebbinghaus, S., Gokhale, V., and Hurley, L. H. (2008) The proximal promoter region of the human vascular endothelial growth factor gene has a G-quadruplex structure that can be targeted by G-quadruplex-interactive agents. *Mol. Cancer Ther. 7*, 880−889.
(25) Cogoi, S., and Xodo, L. E. (2006) G-quadruplex formation within the promoter of the KRAS proto-oncogene and its effect on transcription. *Nucleic Acids Res. 34*, 2536−2549.
(26) Fleming, A. M., Ding, Y., and Burrows, C. J. (2017) Oxidative DNA damage is epigenetic by regulating gene transcription via base excision repair. *Proc. Natl. Acad. Sci. U. S. A. 114*, 2604−2609.
(27) Fleming, A. M., Zhu, J., Howpay Manage, S. A., and Burrows, C. J. (2019) Human NEIL3 Gene Expression Regulated by Epigenetic-Like Oxidative DNA Modification. *J. Am. Chem. Soc. 141*, 11036−11049.
(28) Taneja, P., Gu, J., Peng, R., Carrick, R., Uchiumi, F., Ott, R. D., Gustafson, E., Podust, V. N., and Fanning, E. (2002) A dominant-negative mutant of human DNA helicase B blocks the onset of chromosomal DNA replication. *J. Biol. Chem. 277*, 40853−40861.
(29) Gerhardt, J., Guler, G. D., and Fanning, E. (2015) Human DNA helicase B interacts with the replication initiation protein Cdc45 and facilitates Cdc45 binding onto chromatin. *Exp. Cell Res. 334*, 283−293.
(30) Gu, J., Xia, X., Yan, P., Liu, H., Podust, V. N., Reynolds, A. B., and Fanning, E. (2004) Cell cycle-dependent regulation of a human DNA helicase that localizes in DNA damage foci. *Mol. Biol. Cell 15*, 3320−3332.
(31) Tkac, J., Xu, G., Adhikary, H., Young, J. T. F., Gallo, D., Escribano-Diaz, C., Krietsch, J., Orthwein, A., Munro, M., Sol, W., Al-Hakim, A., Lin, Z. Y., Jonkers, J., Borst, P., Brown, G. W., Gingras, A. C., Rottenberg, S., Masson, J. Y., and Durocher, D. (2016) HELB Is a Feedback Inhibitor of DNA End Resection. *Mol. Cell 61*, 405−418.
(32) Su, N., Byrd, A. K., Bharath, S. R., Yang, O., Jia, Y., Tang, X., Ha, T., Raney, K. D., and Song, H. (2019) Structural basis for DNA unwinding at forked dsDNA by two coordinating Pif1 helicases. *Nat. Commun. 10*, 5375.
(33) Zafar, M. K., Maddukuri, L., Ketkar, A., Penthala, N. R., Reed, M. R., Eddy, S., Crooks, P. A., and Eoff, R. L. (2018) A Small-Molecule Inhibitor of Human DNA Polymerase η Potentiates the Effects of Cisplatin in Tumor Cells. *Biochemistry 57*, 1262−1273.
(34) Arrigo, C. J., Singh, K., and Modak, M. J. (2002) DNA polymerase I of Mycobacterium tuberculosis: Functional role of a conserved aspartate in the hinge joining the M and N helices. *J. Biol. Chem. 277*, 1653−1661.
(35) Schmittgen, T. D., and Livak, K. J. (2008) Analyzing real-time PCR data by the comparative CT method. *Nat. Protoc. 3*, 1101−1108.
(36) Uchiumi, F., Arakawa, J., Iwakoshi, K., Ishibashi, S., and Tanuma, S. (2016) Characterization of the 5′-flanking region of the human DNA helicase B (HELB) gene and its response to trans-Resveratrol. *Sci. Rep. 6*, 24510.
(37) Ducani, C., Bernardinelli, G., Hogberg, B., Keppler, B. K., and Terenzi, A. (2019) Interplay of Three G-Quadruplex Units in the KIT Promoter. *J. Am. Chem. Soc. 141*, 10205−10213.
(38) Weitzmann, M. N., Woodford, K. J., and Usdin, K. (1996) The development and use of a DNA polymerase arrest assay for the evaluation of parameters affecting intrastrand tetraplex formation. *J. Biol. Chem. 271*, 20958−20964.
(39) Han, H., Hurley, L. H., and Salazar, M. (1999) A DNA polymerase stop assay for G-quadruplex-interactive compounds. *Nucleic Acids Res. 27*, 537−542.
(40) Van Houten, B., Santa-Gonzalez, G. A., and Camargo, M. (2018) DNA repair after oxidative stress: Current challenges. *Curr. Opin. Toxicol. 7*, 9−16.
(41) Bokhari, B., and Sharma, S. (2019) Stress Marks on the Genome: Use or Lose? *Int. J. Mol. Sci. 20*, 364.
(42) Redstone, S. C. J., Fleming, A. M., and Burrows, C. J. (2019) Oxidative Modification of the Potential G-Quadruplex Sequence in the *PCNA* Gene Promoter Can Turn on Transcription. *Chem. Res. Toxicol. 32*, 437−446.
(43) Antoniali, G., Lirussi, L., D'Ambrosio, C., Dal Piaz, F., Vascotto, C., Casarano, E., Marasco, D., Scaloni, A., Fogolari, F., and Tell, G. (2014) SIRT1 gene expression upon genotoxic damage is regulated by APE1 through nCaRE-promoter elements. *Mol. Biol. Cell 25*, 532−547.
(44) Fleming, A. M., and Burrows, C. J. (2017) 8-Oxo-7,8-dihydroguanine, friend and foe: Epigenetic-like regulator versus initiator of mutagenesis. *DNA Repair 56*, 75−83.
(45) Spiegel, J., Adhikari, S., and Balasubramanian, S. (2020) The Structure and Function of DNA G-Quadruplexes. *Trends Chem. 2*, 123−136.
(46) Brooks, T. A., and Hurley, L. H. (2009) The role of supercoiling in transcriptional control of MYC and its importance in molecular therapeutics. *Nat. Rev. Cancer 9*, 849−861.
(47) Kan, Z.-Y., Lin, Y., Wang, F., Zhuang, X.-Y., Zhao, Y., Pang, D.-W., Hao, Y.-H., and Tan, Z. (2007) G-quadruplex formation in human telomeric (TTAGGG) 4 sequence with complementary strand in close vicinity under molecularly crowded condition. *Nucleic Acids Res. 35*, 3646−3653.
(48) Gray, L. T., Vallur, A. C., Eddy, J., and Maizels, N. (2014) G quadruplexes are genomewide targets of transcriptional helicases XPB and XPD. *Nat. Chem. Biol. 10*, 313−318.
(49) Fleming, A. M., Zhu, J., Ding, Y., and Burrows, C. J. (2017) 8-Oxo-7,8-dihydroguanine in the Context of a Gene Promoter G-Quadruplex Is an On-Off Switch for Transcription. *ACS Chem. Biol. 12*, 2417−2426.
(50) Fleming, A. M., Zhu, J., Ding, Y., and Burrows, C. J. (2019) Location dependence of the transcriptional response of a potential G-

https://dx.doi.org/10.1021/acs.biochem.0c00218
Biochemistry 2020, 59, 2401−2409

quadruplex in gene promoters under oxidative stress. *Nucleic Acids Res. 47*, 5049−5060.
(51) Kim, N. (2019) The Interplay between G-quadruplex and Transcription. *Curr. Med. Chem. 26*, 2898−2917.
(52) Belotserkovskii, B. P., Soo Shin, J. H., and Hanawalt, P. C. (2017) Strong transcription blockage mediated by R-loop formation within a G-rich homopurine-homopyrimidine sequence localized in the vicinity of the promoter. *Nucleic Acids Res. 45*, 6589−6599.
(53) Dai, J., Dexheimer, T. S., Chen, D., Carver, M., Ambrus, A., Jones, R. A., and Yang, D. (2006) An Intramolecular G-Quadruplex Structure with Mixed Parallel/Antiparallel G-Strands Formed in the Human BCL-2 Promoter Region in Solution. *J. Am. Chem. Soc. 128*, 1096−1098.
(54) Onyshchenko, M. I., Gaynutdinov, T. I., Englund, E. A., Appella, D. H., Neumann, R. D., and Panyutin, I. G. (2009) Stabilization of G-quadruplex in the BCL2 promoter region in double-stranded DNA by invading short PNAs. *Nucleic Acids Res. 37*, 7570−7580.
(55) Morgan, R. K., Batra, H., Gaerig, V. C., Hockings, J., and Brooks, T. A. (2016) Identification and characterization of a new G-quadruplex forming region within the kRAS promoter as a transcriptional regulator. *Biochim. Biophys. Acta, Gene Regul. Mech. 1859*, 235−245.
(56) Palumbo, S. M. L., Ebbinghaus, S. W., and Hurley, L. H. (2009) Formation of a unique end-to-end stacked pair of G-quadruplexes in the hTERT core promoter with implications for inhibition of telomerase by G-quadruplex-interactive ligands. *J. Am. Chem. Soc. 131*, 10878−10891.
(57) Guédin, A., Gros, J., Alberti, P., and Mergny, J. L. (2010) How long is too long? Effects of loop size on G-quadruplex stability. *Nucleic Acids Res. 38*, 7858−7868.
(58) Lane, A. N., Chaires, J. B., Gray, R. D., and Trent, J. O. (2008) Stability and kinetics of G-quadruplex structures. *Nucleic Acids Res. 36*, 5482−5515.
(59) Tippana, R., Xiao, W., and Myong, S. (2014) G-quadruplex conformation and dynamics are determined by loop length and sequence. *Nucleic Acids Res. 42*, 8106−8114.
(60) Gray, R. D., Trent, J. O., and Chaires, J. B. (2014) Folding and unfolding pathways of the human telomeric G-quadruplex. *J. Mol. Biol. 426*, 1629−1650.
(61) Marchand, A., and Gabelica, V. (2016) Folding and misfolding pathways of G-quadruplex DNA. *Nucleic Acids Res. 44*, 10999−11012.
(62) Matsuoka, S., Ballif, B. A., Smogorzewska, A., McDonald, E. R., Hurov, K. E., Luo, J., Bakalarski, C. E., Zhao, Z., Solimini, N., Lerenthal, Y., Shiloh, Y., Gygi, S. P., and Elledge, S. J. (2007) ATM and ATR substrate analysis reveals extensive protein networks responsive to DNA damage. *Science 316*, 1160−1166.
(63) Akimov, V., Barrio-Hernandez, I., Hansen, S. V. F., Hallenborg, P., Pedersen, A. K., Bekker-Jensen, D. B., Puglia, M., Christensen, S. D. K., Vanselow, J. T., Nielsen, M. M., Kratchmarova, I., Kelstrup, C. D., Olsen, J. V., and Blagoev, B. (2018) Ubisite approach for comprehensive mapping of lysine and n-terminal ubiquitination sites. *Nat. Struct. Mol. Biol. 25*, 631−640.
(64) Udeshi, N. D., Svinkina, T., Mertins, P., Kuhn, E., Mani, D. R., Qiao, J. W., and Carr, S. A. (2013) Refined preparation and use of anti-diglycine remnant (k-ε-gg) antibody enables routine quantification of 10,000s of ubiquitination sites in single proteomics experiments. *Mol. Cell. Proteomics 12*, 825−831.
(65) Shiromizu, T., Adachi, J., Watanabe, S., Murakami, T., Kuga, T., Muraoka, S., and Tomonaga, T. (2013) Identification of missing proteins in the neXtProt database and unregistered phosphopeptides in the phosphositeplus database as part of the chromosome-centric human proteome project. *J. Proteome Res. 12*, 2414−2421.

https://dx.doi.org/10.1021/acs.biochem.0c00218
Biochemistry 2020, 59, 2401−2409